Microstructure evolution and texture development of hot form-quench (HFQ) AZ31 twin roll cast (TRC) magnesium alloy

J. Alias, X. Zhou, Sanjeev Das, Omer El-Fakir, and G. E. Thompson

Citation: AIP Conference Proceedings **1901**, 130005 (2017);
View online: https://doi.org/10.1063/1.5010565
View Table of Contents: http://aip.scitation.org/toc/apc/1901/1
Published by the American Institute of Physics

Microstructure Evolution and Texture Development of Hot Form-Quench (HFQ) AZ31 Twin Roll Cast (TRC) Magnesium Alloy

J. Alias[1, a)], X. Zhou[2, b)], Sanjeev Das[3, c)], Omer El-Fakir[4, d)] and G. E Thompson[2, e)]

[1]*Faculty of Mechanical Engineering, Universiti Malaysia Pahang, 26600 Pekan, Pahang, Malaysia*
[2]*Corrosion and Protection Centre, School of Materials, The University of Manchester, M1 3BB, UK*
[3]*Brunel Centre of Advance Solidification Technology, Brunel University, UB8 3PH, UK*
[4]*Department of Mechanical Engineering, Imperial College London, SW7 2AZ, UK*

[a)]Corresponding author: juliawati@ump.edu.my
[b)]x.zhou@manchester.ac.uk
[c)]sanjeevdas80@gmail.com
[d)]omar.al-fakir07@imperial.ac.uk
[e)]george.thompson@manchester.ac.uk

Abstract. The present study on the microstructure evolution of hot form-quench (HFQ) AZ31 twin roll cast magnesium alloy attempt to provide an understanding on the grain structure and heterogeneous intermetallic phase formation in the alloy and texture development following the HFQ process. Grain recrystallization and partial dissolution of eutectic β-$Mg_{17}Al_{12}$ phase particles were occurred during the solution heat treatment at 450°C, leaving the alloy consists of recrystallized grains and discontinuous or random β-$Mg_{17}Al_{12}$ phase particles distribution with small volume fraction. The particles act as effective nucleation sites for new grains during recrystallization and variation of recrystallization occurrence contributed to texture alteration. The partial or full β-$Mg_{17}Al_{12}$ phase dissolution following the HFQ induces void formation that act as fracture nucleation site and the corresponding texture alteration in the recrystallized grains led to poor formability in TRC alloy.

INTRODUCTION

Magnesium is the lightest of all metals used as the basis for engineering alloys. Magnesium could save a considerable amount of vehicle mass, thus promoting energy efficient transportation. The high strength-to-weight ratio of magnesium alloys has drawn the attention of many industries especially the automotive, aerospace and electronics industries. The hexagonal close-packed structure of magnesium and its resultant limitation in easily activated slip systems limits its formability at room temperature. Nevertheless, magnesium alloys can be extremely ductile and easily formable at elevated temperature, which activates its non-basal slip system.

A new technique called hot form-quench (HFQ) has been developed to overcome the formability problem and to improve the mechanical properties of magnesium and aluminium alloys [1-4]. The main feature of the process is to heat the sheet metal to the solution heat treatment (SHT) temperature, at which the ductility is expected to be maximal and to simultaneously form and quench the sheet in a cold die [1,5]. This technique enables the production of magnesium and aluminium parts by rapid processing and also overcomes the springback problem especially in aluminium sheet [2,3,5]. It was suggested that the HFQ process does induce microstructural variation from the solution heat treatment (SHT), forming and rapid quenching [2,6]. The high ductility is expected during the SHT; however, little research is available on the microstructure evolution of the magnesium alloy following the process. Thus, the current study presents the microstructure evolution and texture development of the TRC AZ31 magnesium alloy after the HFQ process. The grain structure development and formation of intermetallic particles were explained based on

Advanced Materials for Sustainability and Growth
AIP Conf. Proc. 1901, 130005-1–130005-6; https://doi.org/10.1063/1.5010565
Published by AIP Publishing. 978-0-7354-1589-8/$30.00

the accompanying electron microscopy. The EBSD map and misorientation profile were also investigated in order to follow the grain structure development.

EXPERIMENTAL

The AZ31 magnesium alloy cast strips (nominal composition of 3.14 wt.% Al, 0.98 wt.% Zn, 0.2816 wt.% Mn, 0.279 wt.% Si, 0.023 wt.% Cu, 0.005 wt.% Ni and Mg balance) with thickness of 1.7 mm were processed in Brunel Centre of Advanced Solidification Technique (BCAST), Brunel University. The strip then underwent the hot form-quench (HFQ) process by Imperial College, London, which included solution heat treatment at 450°C in a furnace, with immediate stamping in a cold die at stamping speed of 250 mm/s and simultaneous cold-die quenching to room temperature [5].

The specimens for microstructure observation were prepared by sectioning the specimen and embedded in hot mounted resin. Care was taken during sectioning of the specimen for longitudinal cross-sectional observation to prevent significant compression during specimen clamping that could affect the grain structure and induced twin formation. Metal clips were used to hold the thin specimen during mounting. Specimens were then mechanically ground with 4000 grit silicon carbide paper, followed by sequential mechanical polishing with 3, 1 and 0.25-micron diamond pastes and finishing with oxide particle suspension (OPS) colloidal silica. The specimens were cleaned with deionized water and ethanol, and quickly dried with a stream of cold air after each grinding stage. Further, the specimens were etched by using the acetic-picral etchant that comprised 5 ml acetic acid, 6 g picric acid, 10 ml water and 100 ml ethanol. The Ultra55 field emission gun-scanning electron microscopy (FEG-SEM) was used to acquire the backscattered diffraction pattern using the charge-coupled device (CCD) camera with a pre-tilted sample stage at 70°. A 20 kV accelerating voltage, 15 mm working distance and spot size 4 were used during the scanning. The diffracted patterns were then acquired using HKL Channel 5 Flamenco software and the EBSD map analysis was acquired using Tango software.

RESULTS AND DISCUSSION

The through-thickness microstructures of the chemically etched as-cast strip and HFQ twin roll cast (TRC) AZ31 magnesium alloys are shown in the optical micrographs in Figure 1 and 2. The etched as-cast alloy specimen displays a coarse dendritic structure, while the HFQ TRC alloy shows a recrystallized grain structure following the microstructure observation. The through-thickness microstructure of the as-cast TRC strip (Figure 1) revealed microstructure variation with finer columnar dendrites evident near the rolled surface (strip edges) in regions I and II, and coarser and compressed columnar dendrites present in the middle of the strip (region III). The red arrow indicates the distribution of second phase particles that can be richly formed at the dendrite boundaries near the strip edges due to the inhomogeneous solidification and deformation during the twin roll casting process [7]. Microsegregation could also be found along the middle region of the TRC strip, which is associated with the non-equilibrium solidification of the alloy. In general, the dendrite orientation of the as-cast alloy depends on the dendrite growth direction during solidification [8].

Figure 2 (a) is the optical micrograph showing through-thickness observation of chemically etched HFQ TRC alloy. The alloy displayed uniform grains throughout the alloy thickness after HFQ. Twins were also present in some of the grains, suggesting that the deformation during HFQ was also accommodated by twinning. The regions of the grains with dark colour are identified as the grains with small volume fractions of β-$Mg_{17}Al_{12}$ phases, that act as particle stimulated nucleation (PSN) for grain nucleation during recrystallization. These regions have different heights than the other grain regions and are known as the first solidified regions during non-equilibrium solidification. These regions were also identified as the dendrite boundaries with network β-$Mg_{17}Al_{12}$ particles in the TRC strip before HFQ. Some of these dark regions also displayed voids due to partial or full dissolution of β-$Mg_{17}Al_{12}$ particles during the HFQ process.

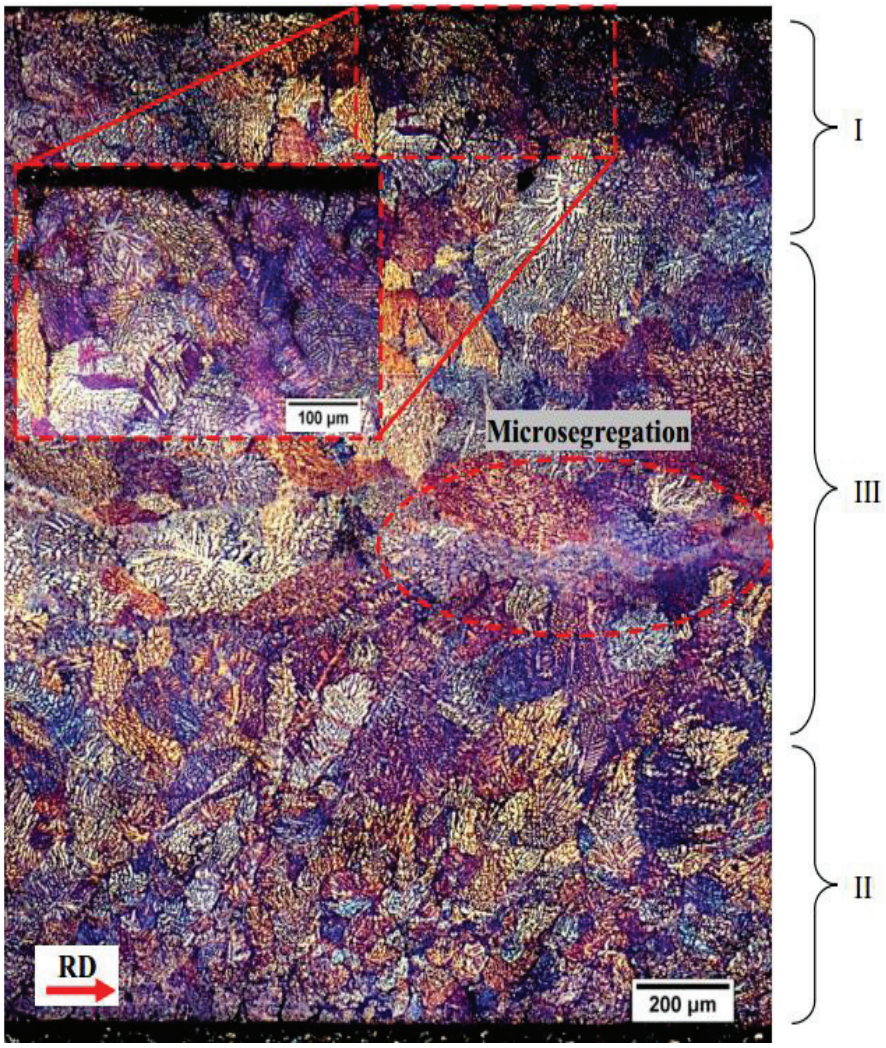

FIGURE 1. Through-thickness microstructure of the etched as-cast TRC AZ31 strip along the casting direction. Regions I and II consist of finer columnar dendrites and region III with coarser and compressed dendrite structure with appearance of microsegregation near the middle of the strip. The red dash box displays the magnified view of region where the second phase particles richly formed near the strip edge in region I.

Figure 2 (b) shows the SEM micrograph of the HFQ TRC AZ31 alloy, which reveals the microstructure of the alloy consists of the α-Mg matrix and bright features dispersed in the alloy. High magnification imaging of the bright features reveals two different types of intermetallic particles, namely the eutectic phases and Mn-rich phases. Further EDX quantitative analysis of the eutectic phases indicated high amounts of Mg, Al and Zn (Table 1), regarded as the $Mg_{17}Al_{12}$ particle. As the cooling rate was relatively high for the alloying elements to adequately diffuse in the solid solution during the solidification process, the solutes (Al and Zn) are enriched in the remnant liquid between the dendrite arms as the dendrites grow and formed the $Mg_{17}Al_{12}$ phase particles [9]. HFQ process significantly changed the β-$Mg_{17}Al_{12}$ phase morphology in the matrix. As the melting point of the β-$Mg_{17}Al_{12}$ phase is at 437°C, the short duration of the heat treatment at 450 °C in the HFQ process lead to dissolution of some of the volume fraction of the particles [1,5,10]. The immediate stamping and cooling down of the stamped alloy after solution heat treatment was insufficient to fully dissolve the particles, and causing these particles to remain in a small volume fraction and randomly distributed in the matrix. The total dissolution of β-$Mg_{17}Al_{12}$ phase particles can take a long duration due to the diffusion rate of aluminium in the magnesium solid state [11]. This condition also promoted voids that are associated with the partial dissolution of the particles, which provide fracture nucleation sites due to the high stress concentration at these region [5,10] and, hence, lead to poor formability of the alloy during the forming process. The

observation of the particle distribution difference is very important since it can be the main factor contributing to the corrosion resistance of the alloy [12–14].

Figure 3 (a) shows the inverse pole figure (IPF) map of the HFQ TRC AZ31 magnesium alloys. Based on the map, the TRC alloy grains were oriented randomly in two different regions of non-basal prismatic and pyramidal orientations, and basal orientation regions after the HFQ process, as marked in the boxes provided in the figure. Such features are occurred due to the non-equilibrium solidification of the TRC alloy and the following HFQ process. The basal orientation occurred in the recrystallized grains from the transformation of the prior dendrite formation during the HFQ process. A similar finding was revealed by Masoumi [7], which indicated that the texture orientation is attributed by the variation occurrence during recrystallization. The earlier recrystallization occurred at the dendrite boundaries with eutectic of β-$Mg_{17}Al_{12}$ phases act as the grain nucleation sites, based on the particle stimulated nucleation (PSN) theory, and thus, the fine recrystallized grains show a preference for non-basal plane orientations and lead to texture alteration.

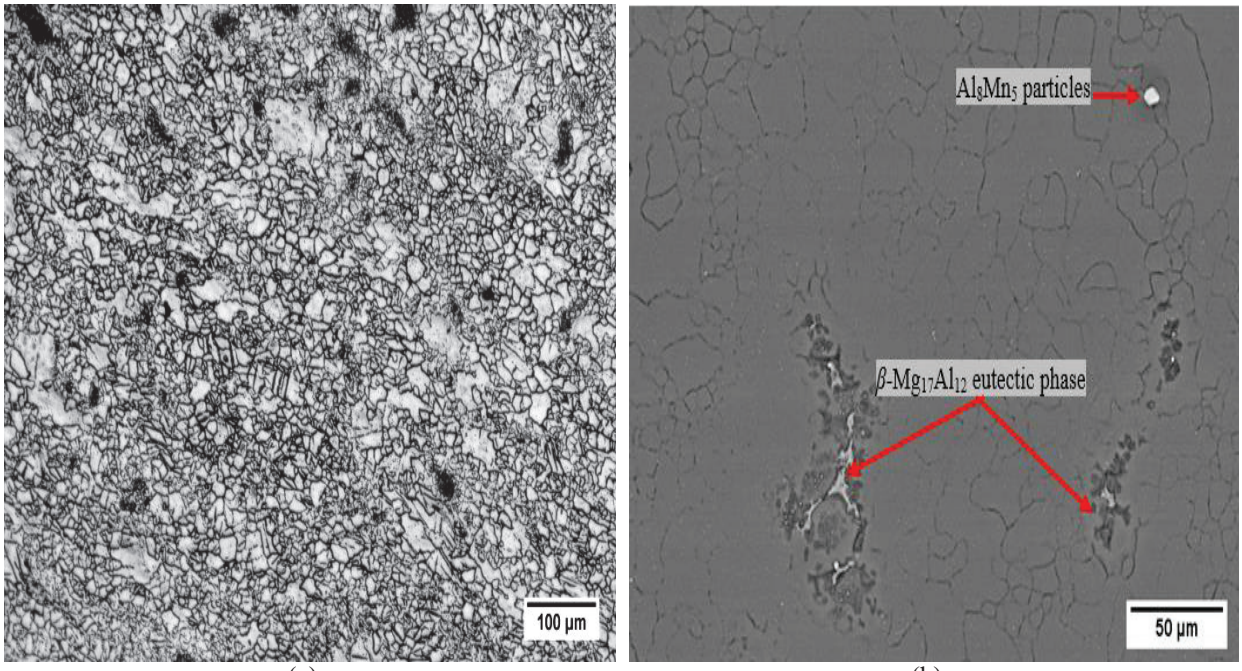

(a) (b)

FIGURE 2. HFQ TRC AZ31 magnesium alloy strip showing (a) through-thickness grain structure; (b) random β-$Mg_{17}Al_{12}$ eutectic particles.

TABLE 1. EDX composition (wt.%) on β-$Mg_{17}Al_{12}$ and Al_8Mn_5 particles.

β-$Mg_{17}Al_{12}$		**Al_8Mn_5**	
Elemen	**Weight%**	**Element**	**Weight%**
C K	4.99	C K	2.80
O K	2.04	Mg K	0.33
Mg K	55.77	Al K	23.72
Al K	17.70	Mn K	72.04
Si K	0.17	Fe K	1.11
Zn K	19.33	Totals	100.00
Totals	100.00		

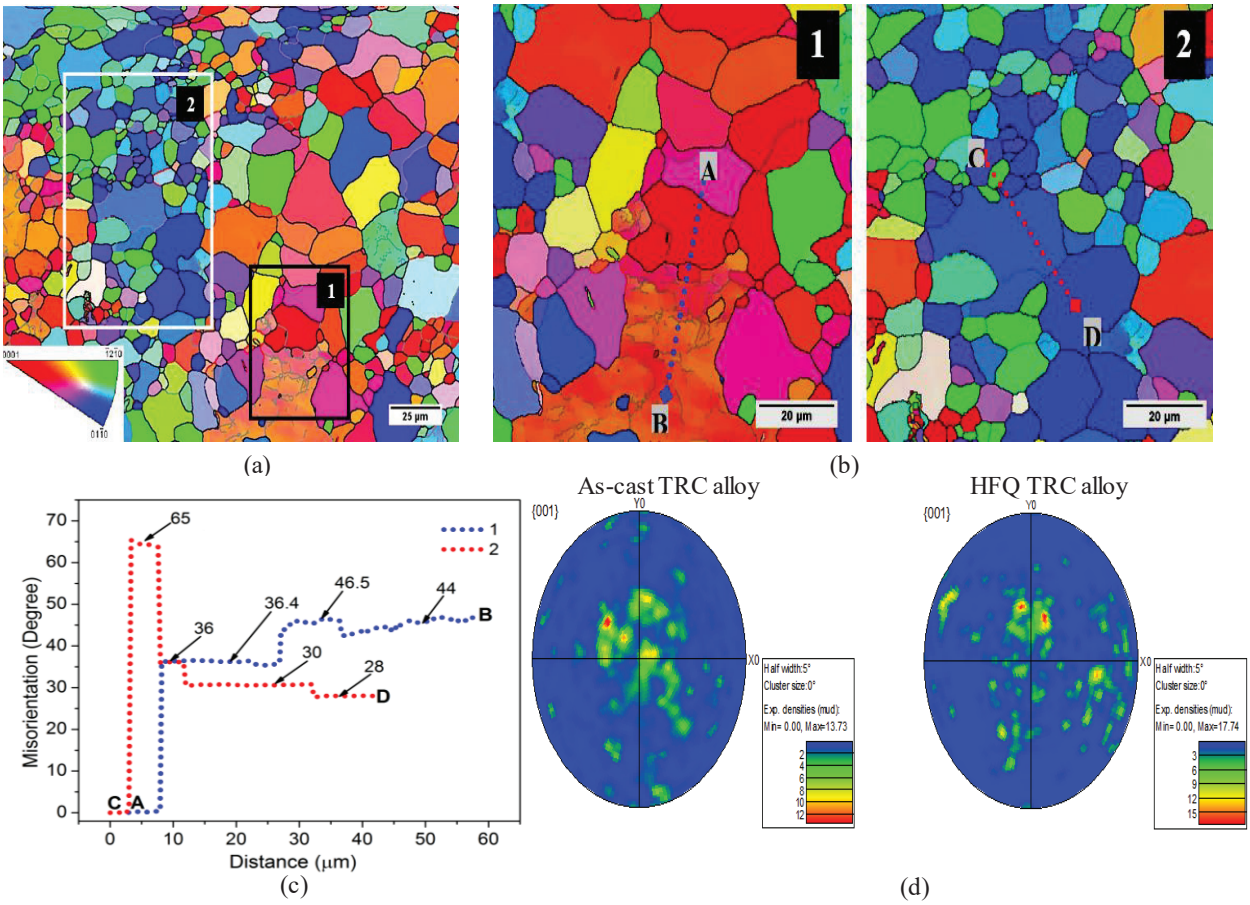

FIGURE 3. Inverse pole figure map of HFQ TRC AZ31 magnesium alloy: a) two different grain preferred orientations (1 and 2); (b) magnified view of two different regions marked as 1 and 2; (c) misorientation profile distribution; and (d) (0002) pole figure of the as-cast and HFQ TRC alloys indicating slight increase in basal texture intensity.

Furthermore, a significant coarse recrystallized grain developed low angle grain boundaries (LAGB) on the dendrite morphology, while, high angle grain boundaries (HAGB) was found develop to the grain itself, as refer to Figure 3(b). Meanwhile, the fine grain region with non-basal prismatic and pyramidal regions is also dominated with HAGB. The misorientation angle profiles taken at recrystallized grains of both regions are evident in Figure 3(c) with most of the fine grains present at around 35° to 45° and the prismatic oriented grains indicated much higher orientation angles at 65°. The pole figures of the TRC AZ31 alloy before and after HFQ are provided in Figure 3(d). The (0002) basal texture shows a weak fibre texture with increased basal intensity from 13.73 to 17.74, after HFQ, which implies insignificant deformation and annealing effect on the texture development. The texture direction also indicated that the dendrites and grains preferentially aligned along the normal direction of the strip and they are distributed in a wide angular range.

CONCLUSIONS

The hot form-quench (HFQ) process has changed the dendrite structure of the TRC strip to recrystallized grains with a coarse dendrite morphology in the alloy surface. The short duration of the solution heat treatment at 450°C in the HFQ process causes the TRC alloy to partially dissolve the β-$Mg_{17}Al_{12}$ phase particles, leaving the particles randomly distributed on the matrix with voids created as fracture nucleation sites and the particles provide particle stimulated grain nucleation (PSN) during recrystallization. Such a condition is attributed to the variation in recrystallization occurrence and random grain orientation and thus, contributed to texture alteration in the HFQ TRC alloy and, consequently, the poor formability in the TRC alloy during forming. Fine recrystallized grains located near

to the β-$Mg_{17}Al_{12}$ phase particles have preferential non-basal prismatic and pyramidal orientations, associated with high angle grain boundaries (HAGB) at around 35 to 45° orientation. Meanwhile, the coarse grains with dendrite morphology have basal orientations and the corresponding dendrite morphology contributed to low angle grain boundaries (LAGB).

ACKNOWLEDGEMENTS

The author would like to thank Teruo Hashimoto for assistance with FEG-SEM image analysis. EPSRC is also thanked for support of the LATEST2 Programme Grant and the TARF-LCV Grant.

REFERENCES

1. R. P. Garrett, J. Lin, and T. A. Dean, Adv. Mater. Res., **6–8** 673–680 (2005).
2. X. Fan, Z. He, S. Yuan, and P. Lin, Mater. Sci. Eng. A, **587** 221–227 (2013).
3. X. Fan, Z. He, S. Yuan, and K. Zheng, Mater. Sci. Eng. A, **573** 154–160 (2013).
4. O. El Fakir, L. Wang, D. Balint, J. P. Dear, J. Lin, and T. a. Dean, Int. J. Mach. Tools Manuf., **87** 39–48 (2014).
5. M. S. Mohamed, A. D. Foster, J. Lin, D. S. Balint, and T. a. Dean, Int. J. Mach. Tools Manuf., **53 (1)** 27–38 (2012).
6. S. Das, N. S. Barekar, O. El Fakir, L. Wang, A. K. Prasada Rao, J. B. Patel, H. R. Kotadia, A. Bhagurkar, J. P. Dear, and Z. Fan, Mater. Sci. Eng. A, **620** 223–232 (2015).
7. M. Masoumi, F. Zarandi, and M. Pekguleryuz, Mater. Sci. Eng. A, **528** 1268–1279 (2011).
8. M. Y. Wang, Y. J. Xu, T. Jing, G. Y. Peng, Y. N. Fu, and N. Chawla, Scr. Mater., **67(7–8)** 629–632 (2012).
9. I. Bayandorian, Y. Huang, Z. Fan, S. Pawar, X. Zhou, and G. E. Thompson, Metall. Mater. Trans. A Phys. Metall. Mater. Sci., **43** 1035–1047 (2012).
10. L. Wang, M. Strangwood, D. Balint, J. Lin, and T.A. Dean, Mater. Sci. Eng. A, **528(6)** 2648–2656 (2011).
11. K. N. Braszczynska-Malik and L. Froyen, *ZEITSCHRIFT FUR Met.*, **96(8)** 913–917 (2005).
12. G.-L. Song, *Corrosion of Magnesium Alloys*. Elsevier (2011).
13. G. L. Makar and J. Kruger, International Materials Reviews, **38(3)** 138–153 (1993).
14. B. Guang, L. Song, and A. Atrens, *Corrosion Mechanisms of Magnesium Alloys,* **1** 11–33 (2000).